

Self-Assembled Microsphere Gratings on Rib Waveguides

Chao-Yi Tai, Bayram Unal, James S. Wilkinson

Optoelectronics Research Centre, University of Southampton, Highfield, Southampton, SO17 1BJ,
United Kingdom
cyt@orc.soton.ac.uk

Mohamed A. Ghanem and Philip N. Bartlett

Chemistry Department, University of Southampton, Highfield, Southampton, SO17 1BJ, United
Kingdom

We report the spectral transmission of a rib waveguide side-coupled to a self-assembled polystyrene microsphere array. A transmission stopband was observed at $\lambda \approx 1590\text{nm}$, showing the potential for realising wavelength-selective devices.

Keywords: self-assembly, distributed feedback, planar lightwave circuits

Introduction

There is ongoing interest in integrating more functionality in planar lightwave circuits (PLCs). Wavelength selective devices are in particularly high demand due to their ability to provide filtering, routing and feedback, which are fundamental requirements for signal processing. Bragg gratings realised in planar waveguides date back to the early 1970's [1] and intensive research on distributed feedback structures has been pursued since then. Photosensitive [2,3] and etched relief gratings [4,5] are presently the most widely used structures. Relief gratings provide greater material flexibility because there is no requirement for special photosensitivity. However, sub-micron scaled patterning and stringent etching tolerances are unavoidable for transferring patterns onto waveguides, resulting in high fabrication costs.

In this paper, we present a promising new technique based upon the combination of self-assembly [6] and conventional photolithography. Sub-micron polystyrene spheres were self-assembled to one side of a photolithographically-defined rib waveguide, forming a linear array. As the spheres are placed against the waveguide, the optical field is drawn out resulting in a strengthened interaction with the spheres. The resultant periodic perturbation of the refractive index experienced by the modal evanescent field leads to coupling to the backward-travelling mode at the Bragg wavelength. The waveguide was designed to be single mode at the wavelength of operation, sufficiently narrow to ensure that a significant proportion of the modal power travelled in the lateral evanescent region, and with a sufficient height to physically trap the microspheres. Polystyrene has a refractive index of approximately 1.59, so that a higher index waveguide material was chosen (Ta_2O_5 ; $n \approx 2$) from which to form the rib waveguides. The great advantage of this configuration is that all the fabrication techniques employed are relatively simple, inexpensive and compatible with existing planar devices which makes this an attractive candidate for scaling up to more sophisticated PLCs. Furthermore, this technique provides a simple route to hybrid circuits combining microspheres in novel functional materials with waveguides in conventional materials.

Fabrication Process

A layer of 500nm thick tantalum pentoxide (Ta_2O_5) was first sputtered from a Ta_2O_5 target in a Ar/O_2 atmosphere onto a Si wafer with $2\mu\text{m}$ SiO_2 buffer layer, with the substrate held at 250°C . The film was then photolithographically patterned with stripes of photoresist of nominal width $1\mu\text{m}$, and argon ion beam milled to transfer the pattern into the Ta_2O_5 resulting in a rib waveguide with an etch depth of 400 nm, and a width of approximately $1.3\mu\text{m}$.

In preliminary work, microspheres were assembled on both sides of the waveguide, but this led to degradation in the effective strength of the grating due to misalignment between the two sides. To avoid such a phase error, we intentionally assembled polystyrene spheres along only one side of the rib waveguide. To achieve this, photoresist was coated over one side of the waveguide surface. A fluidic cell was then assembled by sandwiching a thin frame of Para film (0.5 mm) between the waveguide substrate and a cover glass. A suspension of mono-dispersed polystyrene spheres (1wt%, 499 ± 5 nm in diameter, obtained from Brookhaven) was then injected into the cell with a syringe. The sample was then placed vertically in a temperature-controlled (25°C) incubator, enabling the liquid slug which pushes the polystyrene spheres to sweep across the sample at a speed of 1.5 mm/h during the dewetting process. Once the spheres were physically trapped by the rib waveguide, the capillary immersion force forced the beads to adjust themselves into a well-packed array lined up along the waveguide. When the cell had dried, the sample was heated to 90°C for 1 minute in order to stick the polystyrene spheres to the surface of the waveguide. The remaining photoresist was then removed using 2-propanol, lifting off the microspheres on one side of the rib. A microsphere array of approximately 5mm length was formed along the waveguide. A schematic diagram of the fabrication process sequence is shown in Fig. 1, and a scanning electron micrograph of part of the resultant device is shown in Fig. 2.

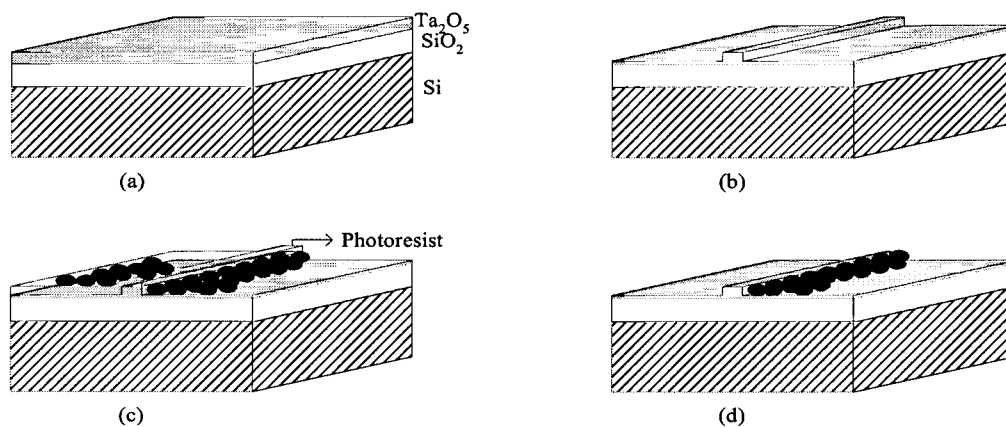


Fig. 1. The fabrication process. (a) Deposit Ta_2O_5 thin film by sputtering. (b) Etch the rib waveguide. (c) Cover one side of the waveguide surface with photoresist and self-assemble the spheres on the surface. (d) Remove the photoresist and fix the spheres in place by thermal annealing.

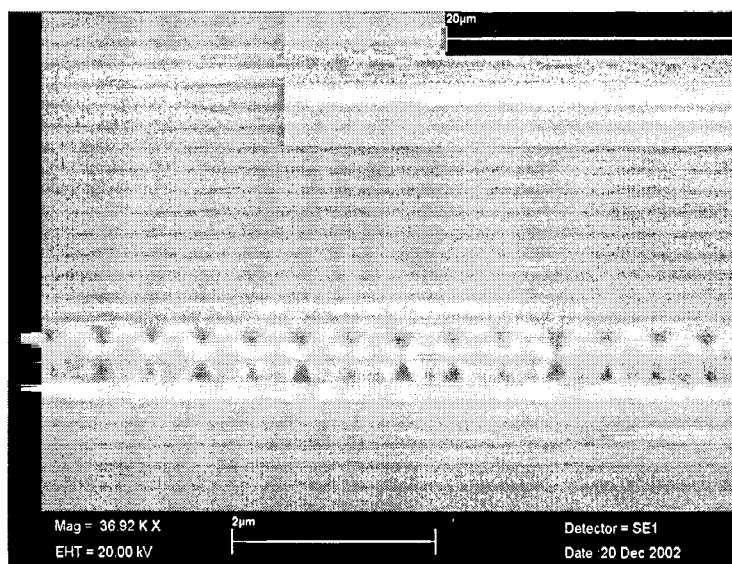


Fig. 2. SEM image of the fabricated sample. The inset details a larger area.

Characterisation and discussion

The transmission spectrum of the sphere-waveguide coupled system was measured using the apparatus shown in Fig. 3. White light from a 150W tungsten lamp was chopped and end-fire launched into a single mode fibre using a 10× microscope objective lens. The fibre was then butt-coupled to the rib waveguide under investigation. The light emerging from the waveguide was collected using a 40× objective lens, passed through a monochromator onto an InGaAs detector, and the signal was fed into a lock-in amplifier and recorded on a computer.

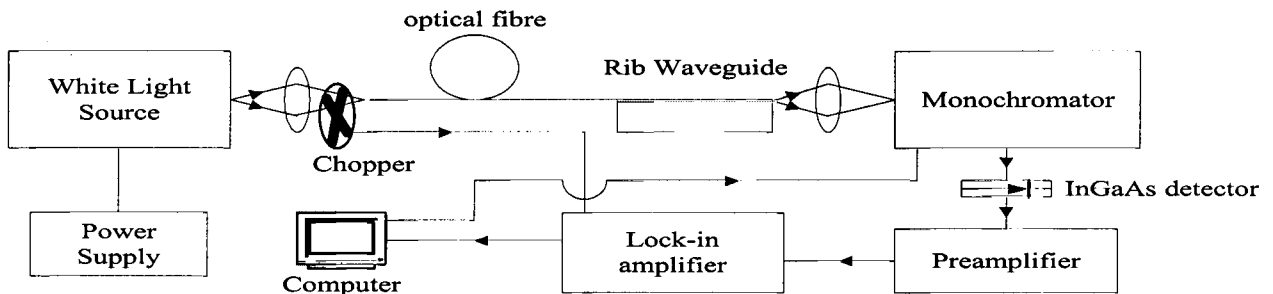


Fig. 3. Experimental arrangement for transmittance measurement.

The transmission spectrum was measured for the same waveguide before assembly of the microspheres and with cladding media of air, water ($n \approx 1.33$) and oil ($n \approx 1.71$) after assembly of the microspheres. Fig. 4 shows the transmission spectra for the three cladding media, normalised to that obtained in the absence of spheres. When the device was surrounded by air, the transmission spectrum shows a notch centred at $\lambda = 1583$ nm with a depth of approximately 0.9 dB (18.7%) and a bandwidth at full width at half maximum power ($\delta\lambda_{FWHM}$) of 16 nm. As the refractive index of the overlay increases to $n = 1.33$ (water), the centre of the stopband shifts to a longer wavelength of $\lambda = 1589$ nm and exhibits a greater depth of 1.55 dB (30%) and a bandwidth $\delta\lambda_{FWHM}$ of 12 nm. Further increase in the refractive index of the cladding medium by using index matching oil ($n = 1.712$) shifts the centre of the stopband to $\lambda = 1596$ nm with a 0.73 dB (15.5%) transmission drop and a bandwidth $\delta\lambda_{FWHM}$ of 14 nm.

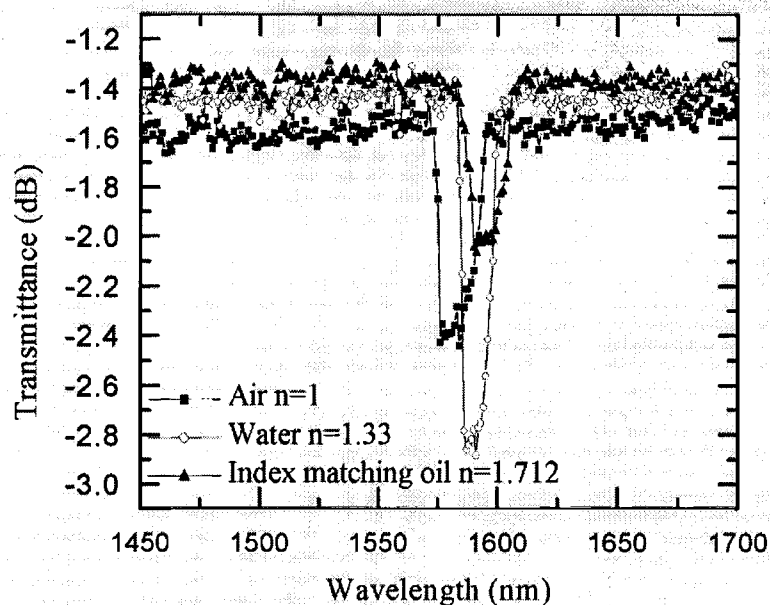


Fig. 4. Transmission spectra for different cladding media.

The reflection wavelength is given by $\lambda_{\text{Bragg}} = 2N_{\text{eff}}\Lambda$, where N_{eff} is the effective refractive index of the waveguide and Λ is the grating period. The value of N_{eff} for the present Ta_2O_5 ($n \sim 2 \pm 0.05$) rib waveguide on a silica substrate ($n \sim 1.46$) is determined by the finite-difference beam propagation method (FD-BPM) to be 1.61 for the case of an air cladding. If it is assumed that the microspheres are well packed, the grating period Λ , is given by the diameter of the polystyrene spheres (499 ± 5 nm). Taking into account the deviation of the particle size and the uncertainty in N_{eff} , Bragg reflection is expected to take place between $\lambda = 1581$ nm to $\lambda = 1613$ nm, which is in close agreement with our experimental results. The shift of the resonant wavelength towards longer wavelengths as the cladding index increases agrees with the expected increase in N_{eff} . The grating strength is dependent upon the index contrast of the periodic perturbation and the overlap of the modal power with the periodic structure. As the index increases from 1.0 to 1.33, the notch in the transmission spectrum deepens, indicating a stronger interaction. This is attributed to the evanescent field extending further into the cladding medium whilst the index contrast between spheres and cladding remains high. A further increase in the cladding index results in reduced grating strength, believed to be due to further field extension being counteracted by the reduced sphere/cladding contrast. The bandwidths of the spectral notches are much greater than would be expected from a weak uniform grating of 5mm length. However, the deviation in the diameters of the spheres, imperfections in the periodicity of the packing and imperfections in the rib waveguide will contribute to this broadening and will also cause a reduction in the depth of the transmission notch. Further investigations of improved sphere diameter control and more uniform assembly are underway.

Conclusions

In conclusion, we have demonstrated a side-coupled rib waveguide microsphere grating using a simple low-cost self-assembly process. The optical coupling between the lateral evanescent field and the self-assembled array results in a stopband in the transmission spectrum, at a wavelength of ≈ 1590 nm, in good agreement with theory. Grating strength adjustment has been examined by varying the refractive index of the overlaid cladding medium, and an extinction of 30% has been obtained. This study demonstrates the potential for self-assembly of microspheres with waveguides for wavelength-dependent devices, and it is expected that this may be extended to microspheres and microsphere resonators of other materials or as part of more sophisticated planar lightwave circuit configurations.

References

- [1] D. C. Flanders, H. Kogelnik, R. V. Schmidt, and C. V. Shank, *Appl. Phys. Lett.* **24**, 194, 1974.
- [2] M. Ibsen, J. Hubner, J. E. Pedersen, R. Kromann, L. -U. A. Andersen, and M. Kristensen, *Electron. Lett.* **35**, 585, 1996.
- [3] D. F. Geraghty, D. Provenzano, W. K. Marshall, S. Honkanen, A. Yariv, and N. Peyghambarian, *Electron. Lett.* **35**, 585, 1999.
- [4] J. E. Román and K. A. Winick, *Appl. Phys. Lett.* **61**, 2744, 1992.
- [5] R. Adar, C. H. Henry, R. C. Kistler, and R. F. Kazarinov, *Appl. Phys. Lett.* **60**, 1779, 1992.
- [6] Yadong Yin, Yu Lu, and Younan Xia, *J. Mater. Chem.*, **11**, 987, 2001.